PERGAMON

International Journal of Solids and Structures 38 (2001) 8879–8897

INTERNATIONAL JOURNAL OF SOLIDS and STRUCTURES

www.elsevier.com/locate/ijsolstr

Dynamic buckling and post-buckling of imperfect columns under fluid–solid interaction

Shijie Cui, Hong Hao *, Hee Kiat Cheong

School of Civil and Structural Engineering, Protective Technology Research Center, Nanyang Technological University, Nanyang Avenue, Singapore 639798, Singapore

Received 3 May 2000; in revised form 7 March 2001

Abstract

Dynamic buckling and post-buckling properties of simply supported imperfect columns under axial fluid–solid interaction are experimentally and numerically investigated in this study. By observing the elastic–plastic responses of imperfect columns, three critical criteria are defined for the columns with prescribed imperfection, namely, the dynamic buckling criterion, the dynamic yielding criterion and the plastic collapse criterion. The relevant critical impulses are determined for each column. The dynamic buckling and collapse mechanism, and the effects of dynamic load duration and initial imperfection of column on the elastic–plastic dynamic buckling and post-buckling properties are examined. The results indicate that, for columns with small imperfection, dynamic buckling will occur with the increase of the fluid–solid impulse. For columns with large imperfection, however, their failure is dominated by the flexural responses. The dynamic buckling and post-buckling characteristics of columns under fluid–solid interaction are also compared and discussed with respect to those of columns under solid–solid impacts. It is found that they are different from those of columns subjected to either impulsive impact or impact owing to suddenly applied load.

Keywords: Dynamic buckling and post-buckling; Initial imperfection; Columns; Fluid–solid interaction

1. Introduction

Dynamic buckling problem of structures has received more and more attention in the last decades because of its broad area of application in many fields of engineering, such as naval architectural engineering, aircraft and aerospace engineering, nuclear power plant engineering and civil engineering. The dynamic buckling of impacted structures can be generally divided into two major categories: dynamic buckling of structures under solid–solid impact and those under fluid–solid interaction. For the solid–solid impacted problem, the dynamic load can be further subdivided into (i) the impact load of large decay rate with short duration, which can be mathematically simplified as an impulsive load so that this kind of dynamic buckling problem is also called "pulse buckling" (Lindberg and Florence, 1987), and (ii) the dynamic load

* Corresponding author. Tel.: +65-791-5278; fax: +65-791-0676.
E-mail address: chhao@ntu.edu.sg (H. Hao).

0020-7683/01/$ - see front matter
PII: S0020-7683(01)00064-6

of small decay rate with long duration, which can be theoretically simplified as a step load with infinite duration.

The earliest study of dynamic buckling of columns subjected to solid–solid impact may be traced back to the investigation by Koning and Taub (1933), who studied the response of a simply supported column subjected to a sudden axial load with a specified duration. They neglected the effect of axial inertia and showed that, when the sudden load is larger than the static critical load, the maximum deflection increases rapidly with time. Since then, many investigations have been conducted on this problem (Lindberg, 1965; Hayashi and Sano, 1972a,b; Lee, 1978; Jones and dos Reis, 1980; Ari-Gur et al., 1982; Gary, 1983; Lindberg and Florence, 1987; Furta, 1990 and Simitses, 1990). More detailed discussions about the dynamic buckling investigations of columns under solid–solid impact can also be referred to Simitses (1987) and Jones (1989, 1996).

For the fluid–solid interaction, dynamic load characteristics are different from those of solid–solid impact (Zhang et al. 1992; Cui et al., 1999). Hence, the dynamic buckling problem of columns under fluid–solid interaction is different from that of columns under solid–solid impact loads. For example, a fluid–solid slamming load has moderate duration, which cannot be simplified as either an impulsive load or a step load with infinite duration. The effect of load duration is important and should be considered in the study of dynamic buckling of structures under fluid–solid interaction. To understand the buckling phenomenon of structures under dynamic loads with moderate duration, Karagiozova and Jones (1992a,b, 1995) investigated the dynamic elastic–plastic buckling of a two-degrees-of-freedom model subjected to a rectangular pulse load and two triangular loads. The analyzed structural model consists of two rigid bars connected by an elastic–plastic spring. Influences of initial imperfection, dynamic load shape and duration, axial inertia and plastic reloading on the dynamic buckling behavior of the model were examined in these studies.

A few studies were carried out on the dynamic buckling of columns subjected to fluid–solid interaction. Zhang et al. (1992) experimentally investigated the dynamic buckling and collapsing of elastic–plastic straight columns under fluid–solid slamming. The boundary conditions of the columns in their study were clamped at both ends. Using the measured axial compressive strains, the authors defined and estimated the critical buckling and plastic peak loading strains of columns. As the plastic collapse of a column usually does not occur at its peak strain (Cui et al., 1999; Karagiozova and Jones, 1996c), the plastic collapse criterion proposed in that study based on the peak strains might underestimate the load bearing capacities of columns. Recently, Cui et al. (1999) studied the dynamic buckling of simply supported straight columns under fluid–solid slamming. Subsequently, a theoretical solution of the buckling of simply supported column to fluid–solid slamming was derived (Hao et al., 2000). A dynamic buckling criterion was defined by means of impulse instead of the peak loading strain as done by Zhang et al. (1992). The dynamic buckling mode of the columns and the effect of slenderness ratio of column were also investigated in the study.

The present paper extends the previous results reported by the authors on straight columns (Cui et al., 1999; Hao et al., 2000). It investigates experimentally and numerically the dynamic buckling and post-buckling properties of imperfect columns subjected to fluid–solid interaction. The primary objectives of the present study are to investigate the dynamic buckling and post-buckling response characteristics of imperfect columns, to define the critical conditions of buckling and plastic collapse, and to evaluate the effect of load duration and initial imperfection of column on the dynamic buckling and post-buckling characteristics.

2. Experimental study

2.1. Specimens and test setting-up

In the present study, 24 imperfect columns with rectangular cross-section were tested. Table 1 lists the length L, the width b, the thickness h and the mass m of the columns. To examine the effect of initial

Table 1
Dimensions, initial imperfection and critical values of imperfect columns

Column no.	Dimensions			m (kg)	$\delta_{0\,\max}$ (mm)	η	Bottom plate	S_{crb} (kg m s^{-1})	$\varepsilon_{\mathrm{c,crb}}$ (μ)	S_{cry} (kg m s^{-1})	$\varepsilon_{\mathrm{c,cry}}$ (μ)	S_{crf} (kg m s^{-1})
	L	b	h									
SIC01	451.4	14.58	9.48	0.487	0.10	1.74	1	1750	415	2160	485	2600
SIC02	451.0	14.39	9.55	0.483	0.40	6.85	1	1460	324	1700	378	1950
SIC03	449.5	14.65	9.64	0.495	0.50	8.38	1	1380	300	1580	365	1770
SIC04	449.8	14.65	9.63	0.495	0.76	12.77	1	1225	268	1350	324	1450
SIC05	449.7	14.69	9.51	0.490	0.78	13.44	1	1190	265	1340	320	1446
SIC06	449.8	14.69	9.56	0.493	0.90	15.34	1	1100	250	1250	318	1350
SIC07	450.6	14.37	9.72	0.491	1.10	18.17	1	980	236	1110	310	1230
SIC08	450.5	14.46	9.50	0.493	1.60	27.67	1	750	199	870	264	1020
SIC09	451.0	14.39	9.53	0.490	1.70	29.24	1			830	263	990
SIC10	449.5	14.41	9.69	0.490	2.00	33.17	1			750	255	930
SIC11	450.2	14.46	9.58	0.486	2.80	47.58	1			670	230	850
SIC12	451.2	14.35	9.70	0.490	3.80	63.12	1			635	212	820
SIC13	451.2	14.50	9.54	0.487	0.11	1.89	2	2120	485	2550	558	3100
SIC14	450.6	14.42	9.38	0.475	0.41	7.27	2	1640	355	1870	426	2250
SIC15	450.2	14.58	9.50	0.437	0.52	8.99	2	1510	330	1700	408	2040
SIC16	450.1	14.76	9.51	0.493	0.75	12.93	2	1268	290	1405	365	1685
SIC17	450.3	14.72	9.48	0.490	0.80	13.89	2	1260	280	1400	360	1680
SIC18	450.2	14.50	9.51	0.482	0.91	15.69	2	1170	273	1300	345	1560
SIC19	450.0	14.43	9.66	0.489	1.12	18.71	2	1035	248	1170	325	1400
SIC20	449.8	14.53	9.39	0.487	1.58	27.92	2	800	215	950	295	1175
SIC21	450.3	14.54	9.59	0.480	1.73	29.34	2			910	286	1140
SIC22	449.7	14.58	9.50	0.486	2.02	34.87	2			830	275	1060
SIC23	450.4	14.52	9.51	0.485	2.82	48.65	2			750	240	960
SIC24	450.8	14.54	9.61	0.491	3.81	64.42	2			700	214	930

Bottom plate 1 – the area is 0.8×0.6 m^2; Bottom plate 2 – the area is 0.8×0.4 m^2.

imperfection on the dynamic buckling and post-buckling properties of columns, the specimens were manufactured to a half-sine initial bending shape, viz., their fundamental bending vibration mode. The maximum initial imperfection, $\delta_{0\,\max}$, and the dimensionless imperfection parameter, η, of each column is also given in the Table, in which $\eta = \lambda\delta_{0\,\max}/h$; $\lambda = 2\sqrt{3}L/h$ is the slenderness ratio of column.

The boundary condition of the columns was simply supported at both ends. By means of a glossy cylinder, the column is connected to the fixtures located on the loading device. When a column is loaded and under bending, the cylinder could rotate freely to simulate a hinge condition. The dynamic responses were measured by strain gauges. The arrangement of strain gauges is shown in Fig. 1. At the loading end of column, two pairs of strain gauges were stuck to measure axial compressive strain and compressive-bending resultant strain, respectively; while only one pair of strain gauges was used to record compressive-bending resultant strain at other measurement points. The specimen material is mild steel. To obtain the properties of the material, five tensile specimens were manufactured and then tested. The average properties are $\varepsilon_{\mathrm{y}} = 1845.5\mu$, $E = 2.11 \times 10^5$ MPa, $\sigma_{\mathrm{ult}} = 569$ MPa and $\varepsilon_{\mathrm{ult}} = 24600.0\mu$.

The tests were carried out at a over-water slamming tower with a special designed loading device. The slamming tower consists of a slamming frame, a slamming traverse girder and a deep pool. The loading device with the column specimen is suspended on the slamming traverse girder. The traverse girder can smoothly move up (lifted by an elevator) and down along sliding guides. The upper end of specimen is connected to the upper supporting boundary of the loading device and the lower end to the lower boundary located on the bottom plate. The bottom plate is separated from the device and can move up and down freely together with the smooth sliding bars. To exam the effect of dynamic load duration on the dynamic

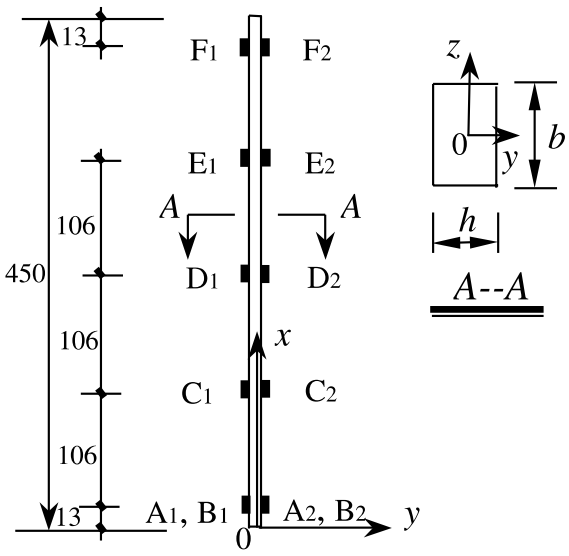

Fig. 1. Arrangement of strain gauges.

buckling and post-buckling properties of imperfect columns, the bottom plate is designed with two different dimensions. One is 0.8 m × 0.6 m, another is 0.8 m × 0.4 m.

The whole testing device is operated by an electromagnetic synchro-control system. In each test, the whole system, including the loading device and transverse girder, is lifted up by an elevator to a certain height and then released by an electromagnetic releaser to allow a free fall. When the loading device slams the water, the speed of the bottom plate will slow down due to its relatively large contact area with water surface, the other part of the loading device will, however, sink into water at a much faster speed. Thus, a fluid–solid interaction load is induced and applied to the column specimen. As a result, the dynamic strains are produced in the column and recorded. At the same time, the impulse, which is a product of the mass of the system and the slamming velocity when the system is about to slam the water surface, is computed. Because the mass of whole moving system, which is about 471 kg for the case when the bottom plate dimensions are 0.8 m × 0.6 m and about 444 kg when the bottom plate is 0.8 m × 0.4 m, is basically unchanged during the tests, the impulse varies with slamming height only. For each column, this test is repeated with different slamming heights from small to large, thus, a series of dynamic responses of the column under different impulses can be obtained. More detailed description on testing devices can be found in a previous paper by the authors (Cui et al., 1999).

2.2. Dynamic responses and buckling of imperfect columns

2.2.1. Fluid–solid slamming load and axial compressive vibration

As mentioned in the previous section, the columns were designed with different initial imperfection to investigate the effect of imperfection of the columns. According to the different dynamic response characteristics, the columns can be divided into two groups, viz., columns with small imperfection and those with large imperfection. Figs. 2 and 3 give the dynamic responses of column SIC04 (small imperfect column) and SIC10 (large imperfect column) under different impulses, respectively, in which ε_c is the axial compressive strain at the slamming end of the specimen, ε_1 and ε_2 are compressive-bending resultant strains on both sides at the middle height of the column, t_P and t_M are the times corresponding to axial compressive

strain peak value and the maximum response of the column, respectively. As can be seen from the figures that the axial compressive strain consists of a main waveform and several smaller waveforms for each slamming. The main waveform is produced by slamming the specimen to water surface, and the following smaller waveforms after t_0 are secondary waves induced from oscillation of the loading device in water after slamming. All the test results, including those of other columns with either bottom plate, which are not shown here, indicate that the secondary waveforms are far smaller than the primary one due to slamming, implying the effects of these secondary waves can be neglected. Therefore, the fluid–solid axial compressive

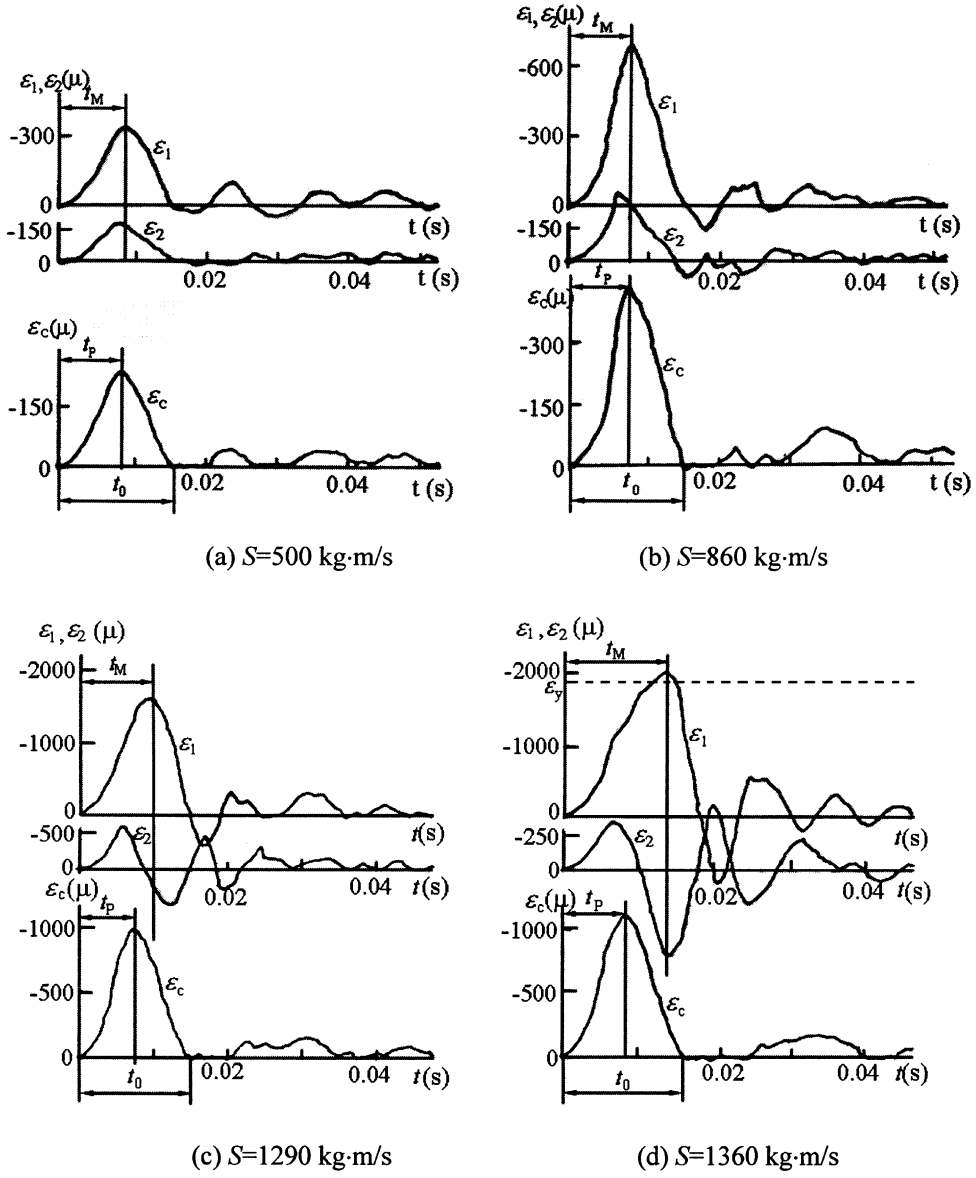

Fig. 2. Dynamic responses of column SIC04 under different impulses.

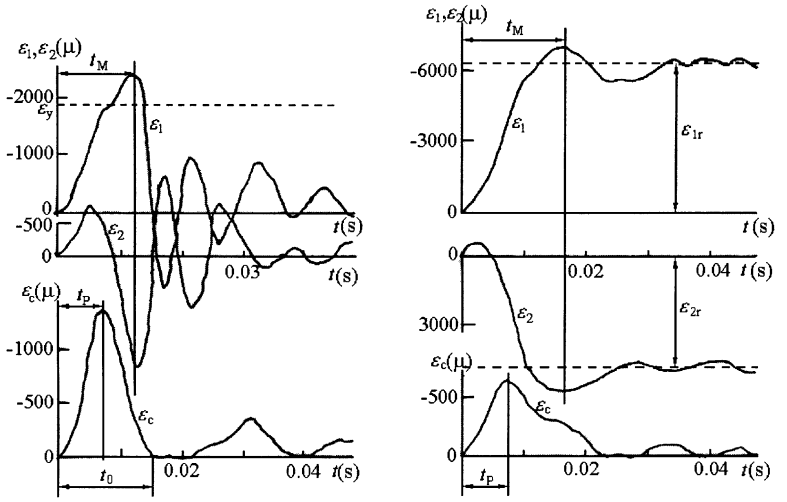

(e) S=1425 kg·m/s (f) S=1450 kg·m/s

Fig. 2 (*continued*)

strains could be approximately simplified as a half-sine wave, where t_0 is the load duration. This observation on the impulse waveform agrees with those obtained by Zhang et al. (1992) for clamped–clamped straight columns and by Cui et al. (1999) for simply supported straight columns. Since these compressive strains are recorded at column end and they are less than the column material yield strain, the fluid–solid slamming induced axial force on the column can be easily estimated by $P(t) = EA\varepsilon(t)$, here E and A are the modulus of elasticity and section area of the column, respectively.

Fig. 4 shows the variation of loading duration t_0 before column collapse versus the maximum imperfection of columns corresponding to two different bottom plates. It indicates that, for a prescribed imperfection, the smaller the bottom plate dimension, the shorter the loading duration. For a given bottom plate, however, the loading duration is basically independent of various impulses and initial imperfection as shown in Figs. 2–4. This implies the loading duration of the tested columns with the same slenderness ratios depends only on the area of bottom plate. This is because a smaller bottom plate will sink into the water faster as compared to a larger bottom plate does, thus the fluid–solid interaction process will be completed faster. As a result, the loading duration corresponding to the fluid–solid interaction is shorter. Moreover, a smaller bottom plate induces less slamming energy due to the shorter loading duration. Therefore, it will need a higher slamming height to induce a larger load value to buckle a column. This observation will be discussed later.

For the columns in the present test, their lengths are about 450 mm, the load duration before the column collapse is 0.015 and 0.012 s for the two different bottom plates, respectively. Thus, axial waves will propagate along the column length back and forth about 138 to 173 times during the load duration. Therefore, the effect of axial inertia on dynamic buckling and flexural response is insignificant for the tested columns under fluid–solid interaction. This is very different from that of solid–solid impacted buckling of columns. For solid–solid impacted columns (high velocity impacted columns), the axial inertia plays an important role in the response of column (Karagiozova and Jones, 1996a,b). It may significantly influence the axial and lateral deformation characteristics, as well as the buckling behavior and the buckling modes of columns. The same observation that the effect of axial inertia is insignificant to dynamic buckling of col-

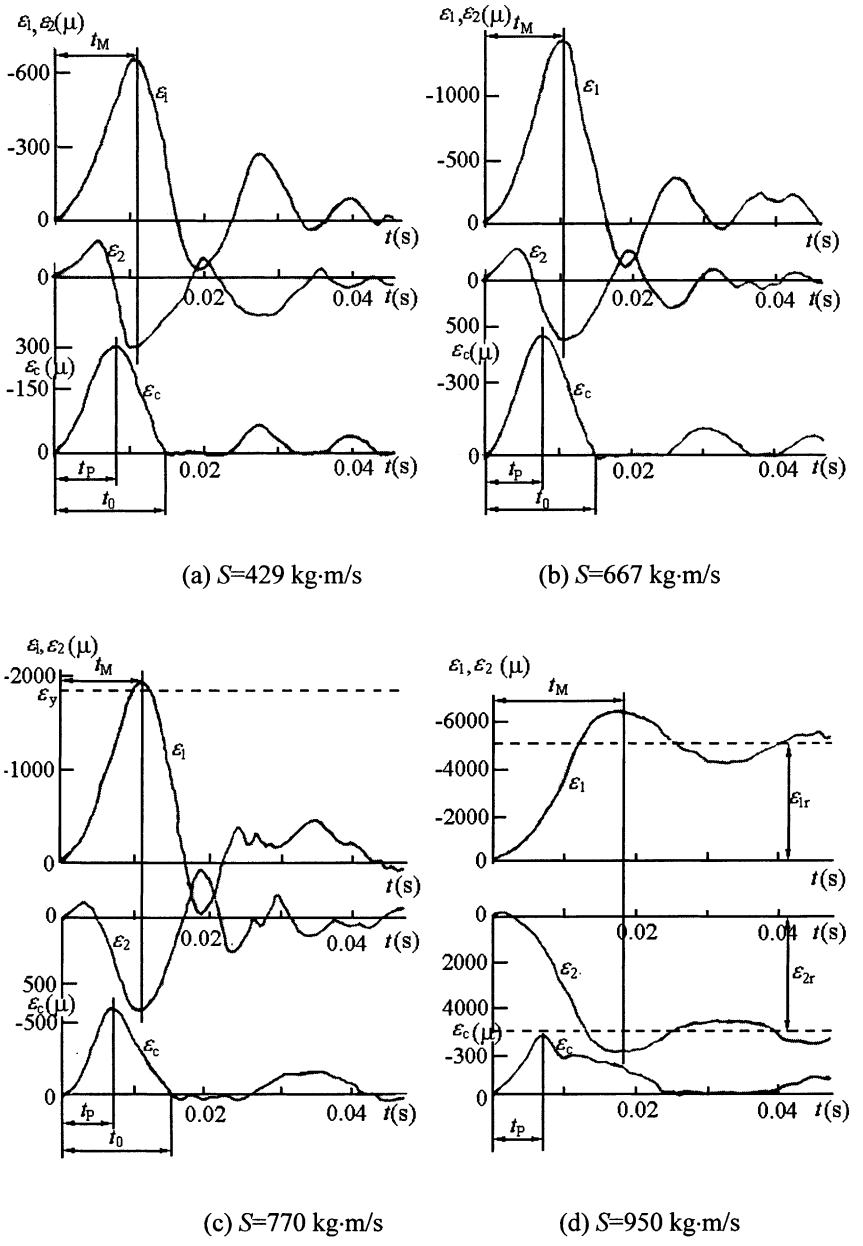

Fig. 3. Dynamic responses of column SIC10 under different impulses.

umns under fluid–solid interaction was also obtained by Zhang et al. (1992) and Cui et al. (1999) for straight columns with both clamped and simply supported boundaries under fluid–solid slamming.

2.2.2. Transverse bending vibration and dynamic buckling criterion

As also can be observed in Figs. 2 and 3, the transverse flexural responses of columns are strongly dependent on impulse S and imperfection of column. For a column with small imperfection (Fig. 2), when

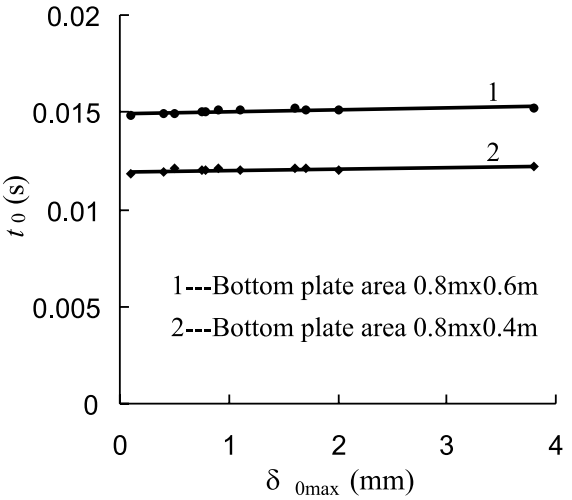

Fig. 4. Variation of loading duration t_0 versus the maximum imperfection of columns.

the impulse is small (e.g. $S = 500\ \mathrm{kg\,m\,s^{-1}}$), the difference of compressive strains on both sides of the column is insignificant, indicating the transverse flexural vibration $[\varepsilon_b = (\varepsilon_1 - \varepsilon_2)/2]$ is insignificant so that the primary response of the column is its axial compressive vibration $[\varepsilon_c = (\varepsilon_1 + \varepsilon_2)/2]$. With the increase of impulse, the bending vibration of the column becomes more and more pronounced (e.g. $S = 860\ \mathrm{kg\,m\,s^{-1}}$). As the impulse increases to $S = 1290\ \mathrm{kg\,m\,s^{-1}}$, the component of transverse flexural vibration becomes larger than that of the axial compressive vibration. This characteristic can be more clearly observed in Fig. 5(a), in which the axial compressive strain $|\varepsilon_c|$, the maximum transverse bending strain $|\varepsilon_b|_{max}$ and the maximum compressive-bending resultant strain $|\varepsilon|_{max}$ are plotted as functions of different slamming im-

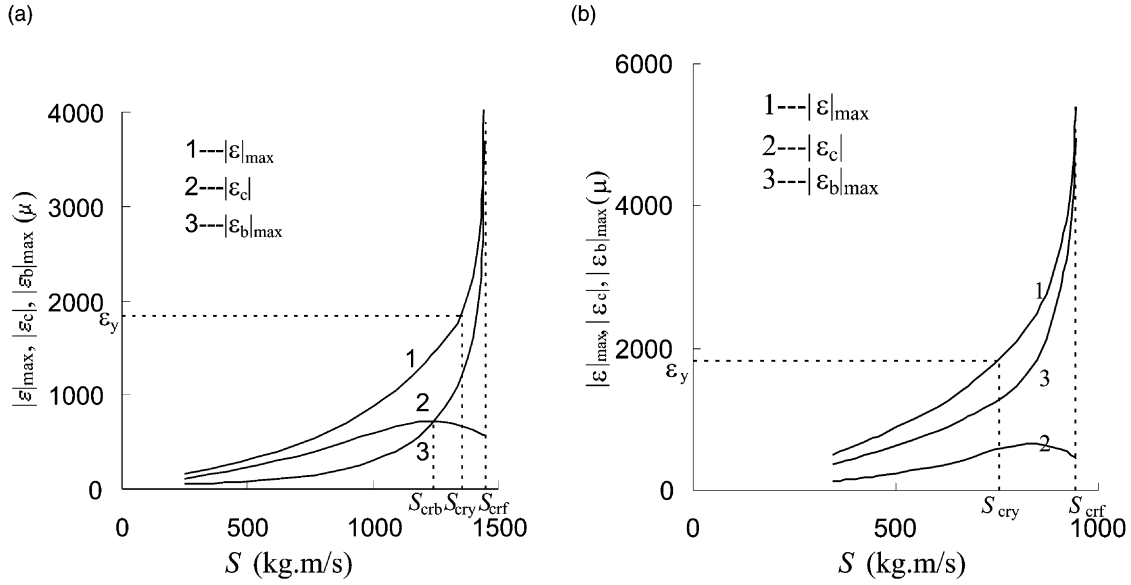

Fig. 5. Determination of critical impulses. (a) Specimen SIC04 and (b) specimen SIC10.

pulses S. This indicates that, for a fluid–solid slammed column with small imperfection, its dynamic response characteristics are dominated by axial compressive vibration when impulse S is small, and dominated by transverse flexural vibration when impulse S is large. According to this observation of the dynamic response characteristics, a dynamic buckling criterion is defined as follows: for a fluid–solid impacted column with a prescribed initial bending imperfection, dynamic buckling is identified to take place when its maximum flexural response is equal to the maximum axial compressive response. The corresponding impulse is defined as the dynamic buckling critical impulse, and denoted by S_{crb}.

For a column with large imperfection, however, the dynamic response characteristics are much different from those of columns with small imperfection. It can be observed from Fig. 3 that the difference between ε_1 and ε_2 is always pronounced, namely, the transverse bending vibration of the column is always larger than its axial compressive vibration even when the impulse is small. This characteristic can also be found in Fig. 5(b). This indicates that the dynamic response characteristic of a column with large imperfection is always dominated by dynamic flexural response. Thus, dynamic buckling will not occur for such columns.

2.2.3. Dynamic buckling mode and buckling mechanism

Fig. 6 shows the distribution of bending strain ε_{b} along the length of column SIC04 under different impulses at the time corresponding to the maximum response ($t = t_{\mathrm{M}}$). It is clear that the lateral responses of column under different slamming loads always have half-sine waveforms. The distributions of ε_{b} for other specimens, which are not shown here, are similar to those of SIC04 illustrated in Fig. 6. This indicates that the dynamic buckling mode of simply supported imperfect columns under fluid–solid interaction is governed by the fundamental vibration mode of column. This is because (i) the initial imperfection of column has the same shape as its fundamental vibration mode, and (ii) the peak loading value of fluid–solid slamming is smaller but its duration is longer as compared to that of solid–solid (high velocity) impact. A load with a small magnitude and long duration is more likely to induce the fundamental vibration mode than a higher mode. This observation agrees with those obtained by Zhang et al. (1992) and Cui et al. (1999).

The dynamic buckling phenomenon of fluid–solid slammed imperfect columns can be explained as follows: for a tested column, besides its initial imperfection, the loading eccentricity is also unavoidable from the loading process. When the column is axially loaded by fluid–solid interaction, both imperfection and loading eccentricity will induce certain transverse flexural vibration besides the axial compressive vibration

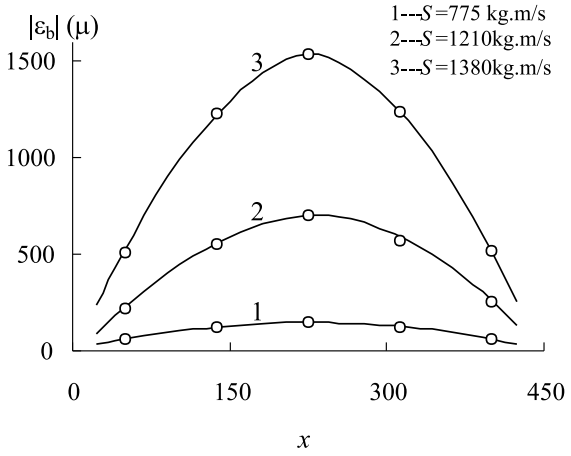

Fig. 6. Distribution of $|\varepsilon_{\mathrm{b}}|$ along the column length.

of the column. For columns with small imperfection, when the impulse is small, the primary response of column is its axial compressive vibration, and the flexural vibration is weak. With the increase of impulse, both axial compressive vibration and flexural vibration increase. However, the flexural vibration of column increases more rapidly because the flexural rigidity of column is much smaller than its axial stiffness. When the impulse reaches the dynamic buckling critical value, the magnitudes of axial compressive vibration and flexural vibration are equal, and the dynamic buckling occurs. For columns with large imperfection, the bending deformation of the column is always larger than its axial compressive deformation during the whole loading process irrespective of the magnitude of impulse. Thus, the response is dominated by the flexural deformation and no dynamic buckling will occur as discussed above.

2.2.4. Plastic response and critical condition for dynamic yielding

As can be seen from Figs. 2 and 3, the dynamic responses of columns increase with the increase of impulse. When the impulse is small, the responses of columns are elastic. When the impulse increases to a certain level, plastic deformation begins to appear in the columns. For example, the elastic–plastic response occurs at the slamming of impulse $S = 1360\ \mathrm{kg\,m\,s^{-1}}$ for specimen SIC04 as shown in Fig. 2 and of $S = 770\ \mathrm{kg\,m\,s^{-1}}$ for SIC10 as shown in Fig. 3. After that, the dynamic responses of columns are elastic–plastic. To separate the elastic and plastic responses of columns, a dynamic yielding condition is defined as: for an imperfect column, the dynamic plastic critical condition is reached when the maximum compressive-bending resultant strain is equal to the material yielding strain. The relevant impulse is defined as the dynamic plastic critical impulse, and denoted as S_{cry}.

2.3. Dynamic post-buckling and collapse of imperfect columns

2.3.1. Dynamic post-buckling responses of columns

Dynamic buckling of a column does not mean losing its load bearing capacity. Reloading buckled columns with different slamming impulses, dynamic post-buckling responses of the columns are obtained. It can be seen from Fig. 2 that, for the column with small imperfection, after dynamic buckling taking place, the maximum transverse bending response does not occur at t_{P} any more. It occurs at a delayed time t_{M}. Nevertheless, t_{M} is always smaller than the loading duration t_0. For the column with large imperfection as shown in Fig. 3, this characteristic can also be observed. This is because the transverse flexural deformation of the column needs a longer time to develop owing to its longer transverse vibration period than the axial vibration period. Hence, unlike the axial vibration, the maximum flexural response occurs after the peak load. On the other hand, the duration of a fluid–solid interaction load is in an order of milliseconds which is much longer than that of a solid–solid impact load (in an order of microseconds) or an impulsive load. The relatively long duration of fluid–solid slamming load allows the transverse flexural deformation of the column to fully develop before the end of the load application, thus, the column may plastically collapse within the loading duration. This is different from plastic collapse of a column under solid–solid impact, in which the maximum transverse flexural response usually occurs after the load application.

As also shown in Figs. 2 and 3, plastic deformations are very large and the plastic residual strains on both sides at mid height of the column, $\varepsilon_{1\mathrm{r}}$ and $\varepsilon_{2\mathrm{r}}$ are also outstanding for these two columns when $S = 1450$ and $950\ \mathrm{kg\,m\,s^{-1}}$, respectively. At these slamming loads, the axial compressive strain recorded at the loading end, namely, the axial impact force, no longer has a half-sine shape. This characteristic is also valid for other tested columns. The same observation was also made by Zhang et al. (1992) for the clamped straight columns under fluid–solid slamming. This indicates that the dynamic post-buckling process of columns under fluid–solid interaction is non-conservative, which is different from that of columns under solid–solid impacts. It is again because of the relatively long loading duration of fluid–solid interaction. When a column is loaded by fluid–solid interaction, plastic deformation occurs within the load duration as

shown in Fig. 2, which results in the reduction of column flexural rigidity. In fact, the dynamic deformation process of the column under present loading can be divided into two stages, namely the elastic reloading stage and plastic response stage. At the first stage of elastic reloading, its flexural rigidity is large and the load carrying capacity is high. Once plastic deformation takes place, the stress flows at a new yielding surface of the column, and its flexural rigidity, as well as its load carrying capacity, decreases. This is often referred to as "soften" of a column. The "soften" of a column causes its effective slenderness ratio to increase. Since increasing the slenderness ratio of a column will make the impact load duration longer (Cui et al., 1999), the impact force in the second plastic response stage has longer duration and smaller magnitude as compared to those in the first elastic response stage. The greater of plastic deformation of the column, the more significant of the change of the impact force shape. When the plastic deformation is fully developed in the column, the fluid–solid slamming load shape is significantly different from that when the response is elastic as shown in Figs. 2 and 3. This is different from the conservative behavior of dynamic post-buckling of columns under solid–solid impact. For solid–solid impact, the load duration is much shorter than that of fluid–solid interaction. The plastic deformations of columns are fully developed only after the dynamic load application. The above observation that the dynamic post-buckling process is non-conservative is an important fact to be noticed since the dynamic post-buckling process of columns under solid–solid impacts is usually conservative.

2.3.2. Plastic collapse critical condition and criterion

As can be seen in Figs. 2, 3 and 5, before the columns collapse, both transverse bending strain and axial compressive strain are growing with the increase of impulse S. When the impulse increases to a certain value, the bending deformation of column increases sharply but the axial compressive strain reduces rapidly with a small increment of impulse. This indicates that the column is losing its load carrying capacity. To estimate the load carrying capacity of columns, a plastic collapse criterion is defined as follows: for a fluid–solid slammed imperfect column, the moment when the flexural deformation increases sharply while the axial compressive strain decreases rapidly with a small increment of impulse is defined as the plastic collapse critical condition of the column. The corresponding impulse is the critical collapse impulse, and denoted as S_{crf}.

2.3.3. Dynamic collapse mechanism of columns

Fig. 7 is a photo of three collapsed specimens. Collapse form for other specimens, which are not shown here, is similar. It can be seen that the collapse of fluid–solid slammed simply supported column is caused by formation of a plastic hinge at the mid height of the column. This is because that the dynamic buckling modes of the columns follow their fundamental transverse vibration shapes, so that the plastic deformation occurs first at mid height of the simply supported columns and then further spreads in both the cross-sectional and axial directions as impulse increases, but the two end parts remain elastic. As a result, the flexural rigidity at mid height of the column is reduced. Consequently, the capacity of bending resistance of the column is weakened. This weakening of the capacity results in the further development of plastic deformations in both the directions from mid height of the column. When the plastic zone develops to an extent that its plastic rigidity becomes a dominant rigidity of the column, a plastic hinge is formed. The slamming energy input is then mainly absorbed by the plastic hinge, while the two end parts of the column become "rigid bars" because their flexural rigidities are basically unchanged. These observations indicate that the dynamic plastic collapse mechanism of columns under fluid–solid interaction is the same as their static plastic collapse mechanism.

2.4. Determination of critical impulses

In the previous discussions, three critical criteria are defined, they are the dynamic buckling criterion, the dynamic yielding criterion and the plastic collapse criterion. For each column, the axial compressive strain

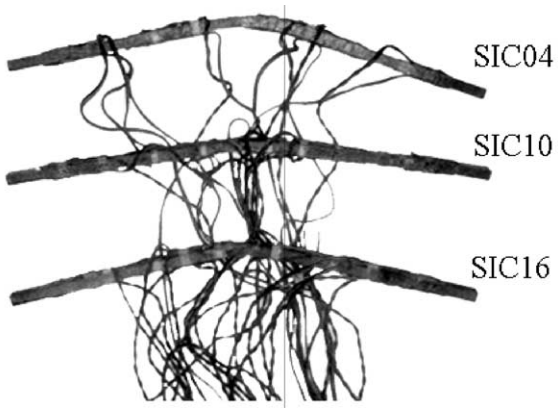

Fig. 7. Collapse mode of columns.

$|\varepsilon_c|$, the maximum transverse bending strain $|\varepsilon_b|_{max}$ and the maximum compressive-bending resultant strain $|\varepsilon|_{max}$ as functions of different slamming impulses S are drawn as shown in Fig. 5. From the critical conditions defined above, three (for the columns with small imperfection) or two (for the columns with large imperfection) critical impulses can be determined for each column. The impulse corresponding to the cross point of $|\varepsilon_c|$ and $|\varepsilon_b|_{max}$ curves is the dynamic buckling critical impulse. The impulse when $|\varepsilon|_{max}$ is equal to the yield strain of column material is the dynamic yielding critical impulse and that corresponding to the approximate vertical asymptotes of $|\varepsilon_c|$ and $|\varepsilon_b|_{max}$ is the plastic collapse critical impulse. The critical impulses determined for the 24 specimens are given in Table 1. Moreover, the critical axial compressive strains corresponding to S_{crb} and S_{cry} are also given in the table, which will be used in the numerical analysis. The maximum axial compressive strain, however, is not given in the table because it does not represent the critical impact load of plastic collapse of the column as discussed in Section 1.

2.5. Effect of duration and initial imperfection of columns

Fig. 8 shows the variation of three critical impulses versus dimensionless imperfection parameter η corresponding to the two duration under consideration. It shows that, as discussed above, the imperfection plays an important role in the dynamic response characteristics of columns. For the tested imperfect columns as shown in Table 1, the columns with small imperfection buckle when dynamic loads are critical, whereas the columns with large imperfection will not buckle but respond laterally to axial impact loads. From the data given in Table 1, columns with $\eta \leqslant 27.92$ will buckle while those with $\eta \geqslant 29.24$ will not. Based on these, an approximate critical dimensionless parameter is estimated as $\eta_{cr} = 28.5$. When $\eta \leqslant 28.5$, dynamic buckling will occur in columns if they are subjected to large enough axial impact loads; when $\eta > 28.5$, however, the dynamic response characteristics of the column is dominated by flexural deformation.

It can also be found from the figure that, for the columns with small imperfection, the dynamic buckling critical load is very sensitive to the initial imperfection. The smaller the initial imperfection, the larger the critical buckling load. Moreover, for the case of $t_0 = 0.012$ s, as imperfection decreases, the buckling load of column increases much faster than that for the case of $t_0 = 0.015$ s. This indicates that, not only the initial imperfection of column has a strong effect on its dynamic buckling properties, but also the load duration will influence the effect of imperfection on dynamic buckling of column. This observation was also made by Karagiozova and Jones (1992a,b) for a two-rigid-bar-spring model. When $\eta > 28.5$, i.e. the initial imperfection is relatively large, the critical impulses for yielding and collapse decrease steadily with increase of

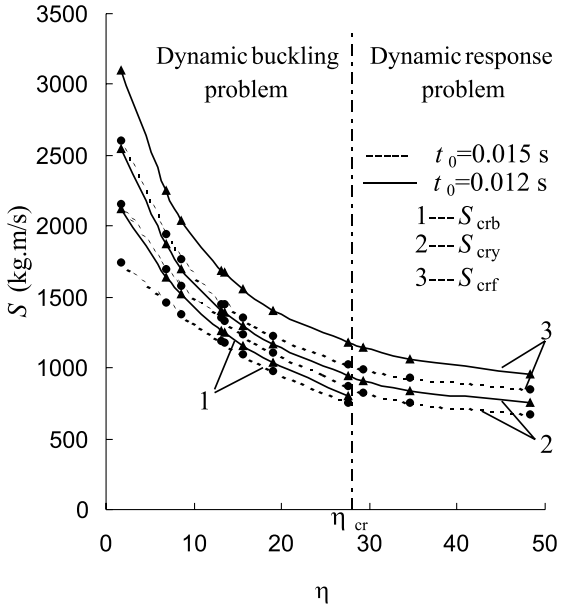

Fig. 8. Effect of duration and initial imperfection of columns.

initial imperfection. When the initial imperfection is small, i.e. $\eta \leqslant 28.5$, however, the critical impulses decrease rapidly as the imperfection increases, implying both the dynamic yielding critical load and the plastic collapse load of columns are also sensitive to the initial imperfection, especially for the case of small imperfection. It also shows that, the critical impulses of columns when duration is $t_0 = 0.012$ s are much larger than those when $t_0 = 0.015$ s. This indicates that both the load duration and imperfection of column will strongly affect the dynamic plastic properties and the load carrying capacities of the columns.

3. Numerical study

A computer program ABAQUS (Hibbit, Karlsson and Sorensen, Inc., 1997) is used for numerical analysis. In finite element modeling, compatible mass matrix and Rayleigh type viscous damping corresponding to the first two modes of the column are adopted. To simulate the deformation of columns, eight-node plane stress element model and large deflection theory are employed by considering the second order terms in strain estimation. In order to describe the non-linear properties of column material, a bi-linear elastic–plastic model is employed in this study. According to the tested column material, the material properties of the model are: elastic modulus $E = 2.11 \times 10^5$ MPa, plastic modulus $E_T = 0.7911 \times 10^4$ MPa and the yield strain $\varepsilon_y = 1845.5\mu$, respectively.

First 12 tested columns are used to calibrate the numerical model. To compare the experimental and numerical results, their dimensions, the maximum initial imperfection $\delta_{0\,max}$ and the corresponding dimensionless imperfection parameter η of the columns are given again in Table 2.

In the present numerical analysis, a series of dynamic responses are calculated for each column by loading the column with different load amplitudes. The impact load is modeled by, $P(t) = P_t \sin(\pi/t_0)t$ when $t < t_0$ and $P(t) = 0$, when $t \geqslant t_0$ in which t_0 is the load duration which has the same value as that from the test.

Table 2
Comparison of numerical and experimental results

Column no.	Dimensions (mm)			$\delta_{0\,max}$ (mm)	η	$P_{t,crb}$ (N)	$P_{t,crb\,E}$ (N)	Error (%)	$P_{t,cry}$ (N)	$P_{t,cry\,E}$ (N)	Error (%)	$P_{t,crf}$ (N)
	L	b	h									
SIC01	451.4	14.58	9.48	0.10	1.74	12650	12103	4.52	15400	14145	8.87	17050
SIC02	451.0	14.39	9.55	0.40	6.85	9800	9395	4.31	12050	10961	9.93	13800
SIC03	449.5	14.65	9.64	0.50	8.38	9250	8940	3.47	11500	10876	5.73	13200
SIC04	449.8	14.65	9.63	0.76	12.77	8200	7978	2.78	10300	9645	6.79	12000
SIC05	449.7	14.69	9.51	0.78	13.44	8120	7811	3.96	10270	9433	8.87	11900
SIC06	449.8	14.69	9.56	0.90	15.34	7700	7408	3.94	9900	9423	5.06	11550
SIC07	450.6	14.37	9.72	1.10	18.17	7150	6955	2.80	9360	9136	2.45	10900
SIC08	450.5	14.46	9.50	1.60	27.67	5900	5768	2.29	8430	7652	10.17	9960
SIC09	451.0	14.39	9.53	1.70	29.24				8300	7610	9.07	9800
SIC10	449.5	14.41	9.69	2.00	33.17				7850	7513	4.49	9400
SIC11	450.2	14.46	9.58	2.80	47.58				7000	6723	4.12	8550
SIC12	451.2	14.35	9.70	3.80	63.12				6510	6226	4.56	7900
						Mean		3.51			6.68	

3.1. Dynamic response characteristics and critical conditions

Fig. 9 shows the strain response time histories of column SIC01 under several load amplitudes when the material damping ratio is $\xi_c = 0.025$, in which ε_1 and ε_2 are the compressive-bending resultant strains on both sides at mid height of the column. Fig. 10 illustrates the numerically calculated maximum strains $\varepsilon_{1\,max}$, $\varepsilon_{2\,max}$, $\varepsilon_{c\,max}$ and $\varepsilon_{b\,max}$ for columns SIC01 and SIC10 under different impact load amplitudes. It should be noted that the numerical results of SIC01, instead of SIC04, are shown here. This is because the dynamic response characteristics of each column are very similar. It should also be noted that the numerical vibration attenuates much slower that that observed in the test because columns actually vibrate in water in the test. This is not modeled in the numerical analysis since only the impact phase is of concerned.

It is observed that the numerical dynamic response characteristics of column are very similar to those obtained from the test. The numerical results show that the maximum strain response always occurs during the load duration t_0, and the dynamic response characteristics are strongly dependent on the initial imperfection of columns and the magnitude of impact load. Also, as observed from the test, for the columns with small imperfection, the dominant dynamic response characteristic of column is qualitatively changed from the axial compressive vibration dominance when the dynamic load is small to the transverse flexural vibration dominance when the dynamic load is large. Moreover, when the dynamic load increases to a certain value, the maximum compressive-bending resultant strain of the column reaches to the yield strain of column material. At another "critical condition", the maximum strain $\varepsilon_{1\,max}$ and $\varepsilon_{2\,max}$ on both sides at mid height of the column increase sharply with a small increment of dynamic load. As a result, the bending strain of the column increases very fast while the axial compressive strain decreases rapidly, implying a plastic hinge is formed at mid height of the column, and the column is losing its load bearing capacity. These observations indicate that the three critical conditions, namely, dynamic buckling, yielding and collapse conditions, as observed in the test results, are also shown in the numerical results. Thus, the criteria defined above can be used to estimate the corresponding critical dynamic loads in numerical analysis. For the columns with large imperfection (e.g. SIC10), however, the change of dominant response from axial to flexural vibration does not exist anymore, and the dominant vibration of the column is always its transverse bending vibration. This indicates again that the failure of columns with large imperfection is dominated by their flexural responses, and the dynamic buckling will never occur. The critical conditions for dynamic yielding and collapse, however, can still be observed from the numerical results for the columns with large imperfection.

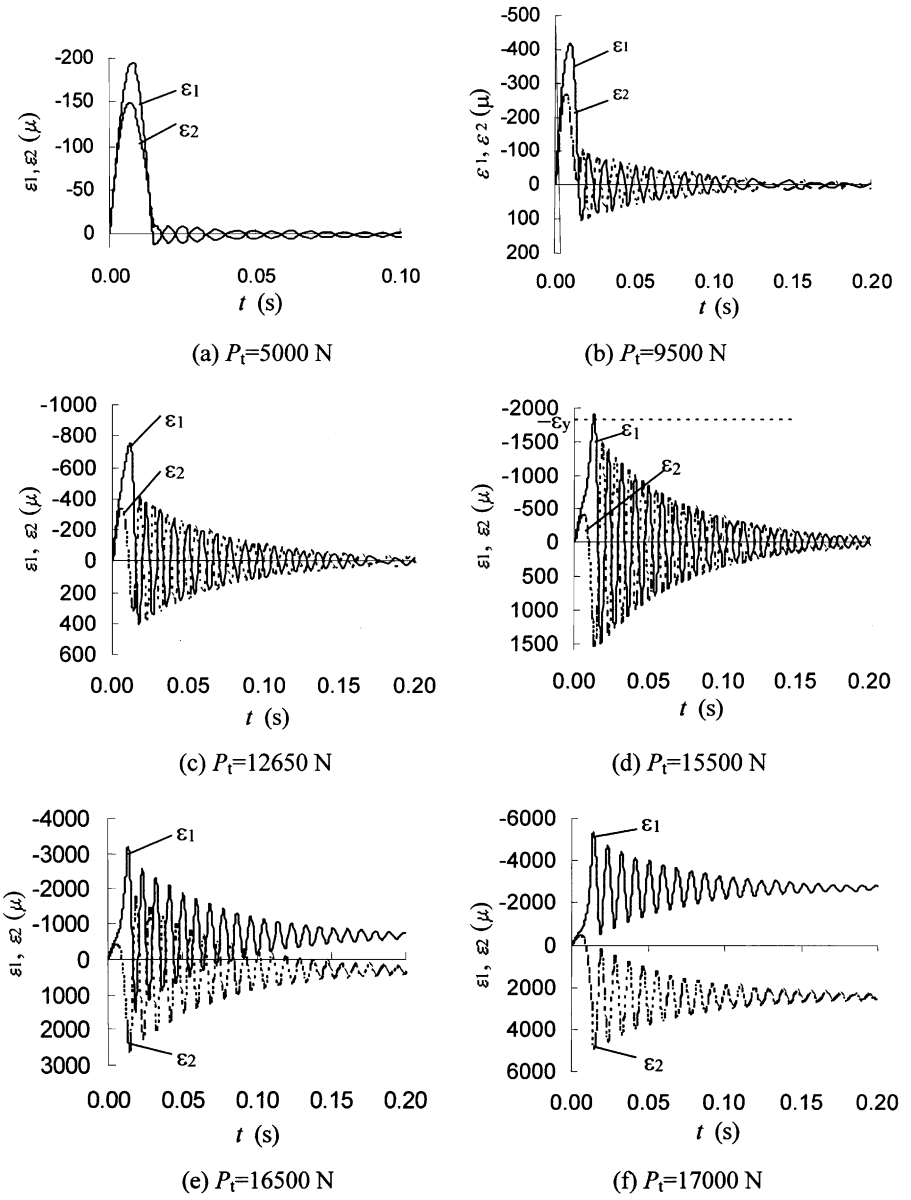

Fig. 9. Dynamic responses of column SIC01 under different dynamic loads.

Fig. 11 shows the transverse displacement response time histories at mid height of the column under three dynamic load amplitudes and the variation of the maximum displacement versus different load amplitudes. In order to show the displacement clearly, the displacements corresponding to $P_t = 5000$ and 9500 N shown in Fig. 11(a) are amplified by 40 times and 15 times, respectively. As can be seen from this figure, when dynamic load is small, the displacement response of the column is small. The transverse displacement increases with the increase of dynamic load amplitude. Fig. 11(b) illustrates the maximum displacement with respect to different load amplitudes. It shows a "knee" at the dynamic buckling critical

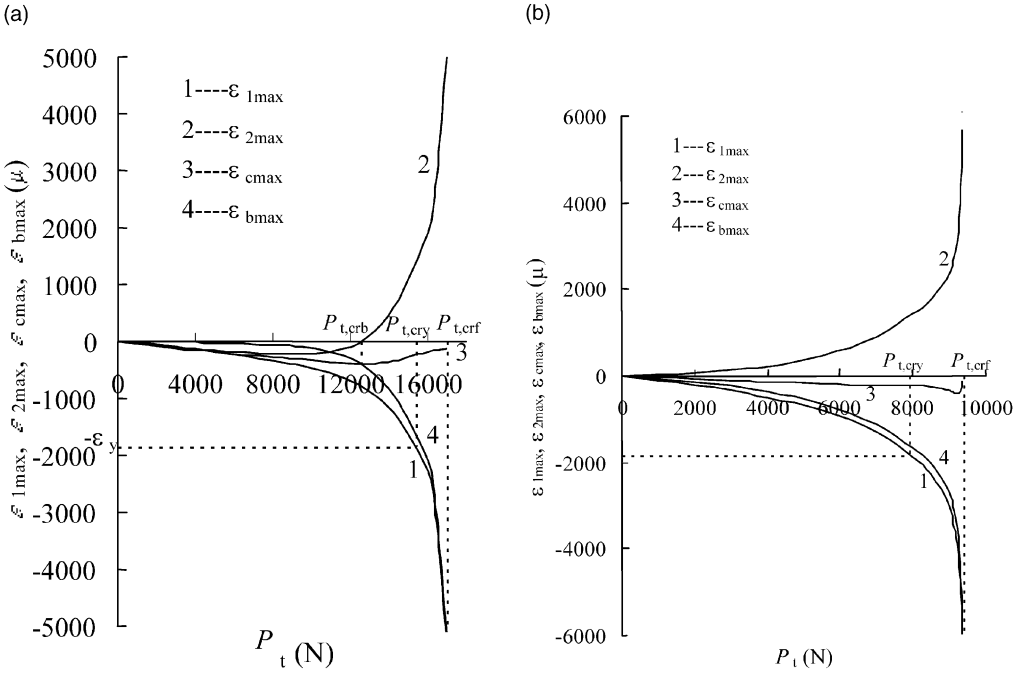

Fig. 10. Variation of $\varepsilon_{1\,max}$, $\varepsilon_{2\,max}$, $\varepsilon_{c\,max}$ and $\varepsilon_{b\,max}$ versus different load amplitudes. (a) Column SIC01 and (b) Column SIC10.

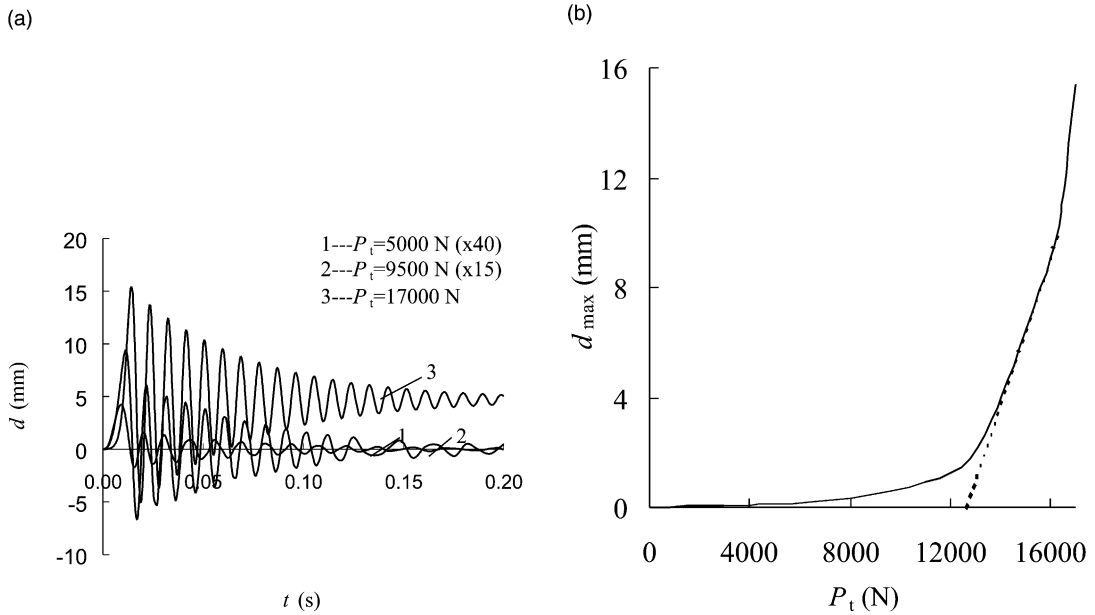

Fig. 11. Displacement responses of column SIC01. (a) Displacement time history and (b) Variation of the maximum displacement versus dynamic loads.

load. When the dynamic load is smaller than this critical load, the slope of the curve is flat, indicating the development of the maximum transverse displacement of the column is steady as the dynamic load increases. When the dynamic load is larger than the critical load, the slope of the curve becomes steep, indicating the transverse displacement of the column increases rapidly for a small increment of the dynamic load after the column buckles.

It can also be found from Fig. 11(b) that, when the dynamic load approaches the load bearing capacity of the column, the curve of the maximum displacement shows another turning point, after that, the displacement increases even faster with the increase of dynamic load. This turning point indicates the dynamic response of the column is dominated by its plastic deformation.

It should be pointed out that, in the experimental study of imperfect columns under fluid–solid interaction, when the dynamic load is close to the plastic collapse critical load, the column reaches to its maximum response at a much delayed time than the peak dynamic load. However, in the present numerical study, the maximum response occurs almost at the same time as the load reaches its peak value as shown in Fig. 9. This is because, as discussed in the experimental study, the dynamic post-buckling process of columns subjected to fluid–solid interaction is non-conservative. The dynamic responses of columns are coupled with the applied dynamic load. When the responses of columns are dominated by their plastic deformation, the dynamic load shape is seriously changed and no longer remains a half-sine waveform. At the same time, its duration becomes much longer. As a result, the maximum response of the column occurs much later than the peak loading time. For the present calculated columns, however, this non-conservative property is not simulated in the numerical study. The dynamic load is always a half-sine waveform with same duration. Therefore, the time corresponding to the maximum response of the column is almost the same as the peak loading time.

3.2. Comparison with the experimental results

Numerical results of the three critical dynamic loads, viz., the dynamic buckling critical load $P_{\mathrm{t,crb}}$, the dynamic yielding critical load $P_{\mathrm{t,cry}}$ and the plastic collapse critical load $P_{\mathrm{t,crf}}$ of the 12 columns are determined and given in Table 2. For comparison, the experimental results of dynamic buckling critical load $P_{\mathrm{t,crb\,E}}$ and the dynamic yielding critical load $P_{\mathrm{t,cry\,E}}$ for the columns are also given in Table 2. It is obvious from the table that the numerical results agree well with the experimental results. The errors are about 2.29–4.52% for the dynamic buckling critical loads with an average error of 3.51%, and about 2.45–10.17% for their dynamic yielding critical loads with an average error of 6.68%. The error between the experimental and numerical results might be attributed to the facts that (1) the impact loads used in this numerical study are not exactly the same as the actual impact loads in the test; and (2) small loading eccentricity is unavoidable for each column in the test, but it is not considered in this numerical study.

It should be pointed out that the plastic collapse critical load could not be determined in the test because, as discussed above, the dynamic post-buckling process of the columns under fluid–solid interaction is non-conservative. When a column collapses, the corresponding dynamic load is seriously twisted. As a result, the dynamic load corresponding to the plastic collapse is not the maximum one. Therefore, the numerical results for plastic collapse critical load are not compared with the experimental results.

3.3. Effect of initial imperfection of column

To investigate the effect of initial imperfection of column on its dynamic buckling critical load, columns with different initial imperfection magnitudes are calculated with different load duration $t_0 = 0.006$, 0.015 and 0.050 s. Fig. 12 shows the variations of dynamic buckling loads of columns versus the initial imperfection. First, it shows that the initial imperfection strongly affects the critical buckling load of columns. The smaller the initial imperfection, the higher the critical buckling load of column. On the other hand, the

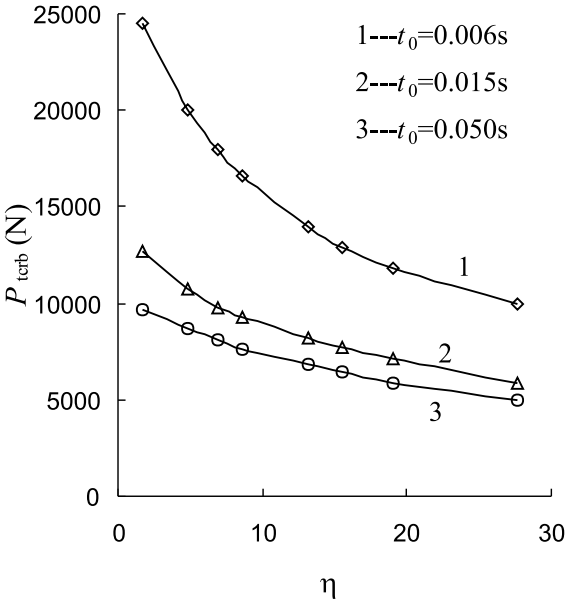

Fig. 12. Effect of initial imperfection ($\lambda = 164$, $\xi_c = 0.025$).

critical buckling load of the column with short load duration increases much faster than that of the column with relatively long load duration as the imperfection decreases. This observation indicates that, as observed by Karagiozova and Jones (1992b) for the dynamic buckling of an idealized "spring-rigid bar" model, the dynamic load duration has a significant influence not only on the dynamic buckling critical load of columns, but also on the sensitivity of the initial imperfection. The sensitivity of the initial imperfection on dynamic buckling load increases as the load duration decreases. This observation is the same as that from the test.

4. Conclusions

Dynamic buckling and post-buckling responses of simply supported imperfect columns under fluid–solid interaction have been analyzed and discussed. Based on the response characteristics, three critical conditions are defined, they are dynamic buckling critical condition, dynamic yielding critical condition and plastic collapse critical condition. According these conditions, three critical impulses (dynamic loads) are estimated experimentally and numerically for each column. Moreover, the effect of dynamic load duration and initial imperfection of column is also investigated in this study. It has been found that

1. The duration of a fluid–solid impact load is in an order of milliseconds. For this kind of load duration, the effect of axial inertia on the dynamic buckling and flexural response of column is insignificant.
2. Initial imperfection plays an important role in the dynamic response characteristics of columns. When $\eta \leqslant 28.5$, dynamic buckling will occur if the impact load is strong enough; when $\eta > 28.5$, however, the response is always dominated by flexural bending such that no dynamic buckling will occur.
3. The dynamic buckling modes of simply supported imperfect columns are governed by their fundamental lateral vibration mode. The collapse of the columns is caused by formation of a plastic hinge at the middle of the column, which is the same as their static plastic collapse form.

4. Because of the relatively long duration of fluid–solid impact load, dynamic post-buckling process of the columns is non-conservative.
5. For columns with small imperfection, the initial imperfection of column has a strong effect on its dynamic buckling properties. The dynamic buckling critical impulse increases rapidly as initial imperfection decreases. The load duration also influences the effect of imperfection on dynamic buckling of column.
6. Both load duration and imperfection of column will strongly affect the critical impulses (dynamic loads) for dynamic yielding and collapse of the columns, especially for the case of small imperfection. The shorter the load duration and smaller the imperfection, the higher the dynamic yielding and the plastic collapse critical impulses (dynamic loads) of the columns.

References

Ari-Gur, J., Weller, T., Singer, J., 1982. Experimental and theoretical studies of columns under axial impact. Int. J. Solids Struct. 18 (7), 619–641.

Cui, S., Cheong, H.K., Hao, H., 1999. Experimental study on dynamic buckling of simply-supported columns under axial slamming. J. Engng. Mech. ASCE 125 (5), 513–520.

Furta, S.D., 1990. Dynamic stability of an elastic column. Appl. Math. Mech. 54 (6), 769–776.

Gary, G., 1983. Dynamic buckling of an elastoplastic column. Int. J. Impact Engng. 1 (4), 357–375.

Hao, H., Cheong, H.K., Cui, S.J., 2000. Dynamic buckling investigation of imperfect columns under intermediate velocity impact. Int. J. Solids Struct. 37, 5297–5313.

Hayashi, T., Sano, Y., 1972a. Dynamic buckling of elastic bars (the case of low velocity impact). Bull. JSME 15 (88), 1167–1175.

Hayashi, T., Sano, Y., 1972b. Dynamic buckling of elastic bars (the case of high velocity impact). Bull. JSME 15 (88), 1176–1184.

ABAQUS Standard User's Manual; Theory Manual; Standard Example Problem Manual, 1997. Hibbit, Karlsson and Sorensen, Inc..

Jones, N., Reis, H.L.M., 1980. On the dynamic buckling of a simple elastic–plastic model. Int. J. Solids Struct. 16, 969–989.

Jones, N., 1989. Recent studies on the dynamic plastic behavior of structures, Appl. Mech. Rev. 42 (4), 95–115.

Jones, N., 1996. Recent studies on the dynamic plastic behavior of structures–An update. Appl. Mech. Rev. 49 (10), S112–S117.

Karagiozova, D., Jones, N., 1992a. Dynamic buckling of a simple elastic–plastic model under pulse loading. Int. J. Non-Linear Mech. 27 (6), 981–1005.

Karagiozova, D., Jones, N., 1992b. Dynamic pulse buckling of a simple elastic–plastic model including axial inertia. Int. J. Solid Struct. 29 (10), 1255–1272.

Karagiozova, D., Jones, N., 1995. Some observation on the dynamic elastic–plastic buckling of a structural model. Int. J. Impact Engng. 16 (4), 621–635.

Karagiozova, D., Jones, N., 1996a. Multi-degrees of freedom model for dynamic buckling of an elastic–plastic structure. Int. J. Solid Struct. 33 (23), 3377–3398.

Karagiozova, D., Jones, N., 1996b. Dynamic elastic–plastic buckling phenomena in a rod due to axial impact. Int. J. Impact Engng. 18 (7–8), 919–947.

Karagiozova, D., Jones, N., 1996c. Dynamic buckling of columns due to slamming loads. International Conference on Structures under Shock and Impact, SUSI. Computational Mechanics Inc., Billerica, MA, USA, pp. 311–320.

Koning, C., Taub, J., 1933. Impact buckling of thin bars in the elastic range hinged at both ends, Luftfahrtforschung 10 (2), pp. 55–64 (translated as NACA TN 748 in 1934).

Lee, L.H.N., 1978. Quasi-bifurcation of rods with an axial plastic compressive wave. J. Appl. Mech. 45, 100–104.

Lindberg, H.E., 1965. Impact buckling of a thin bar. J. Appl. Mech. 32 (2), 315–322.

Lindberg, H.E., Florence, A.L., 1987. Dynamic pulse buckling–Theory and experiment. Martinus Nijhoff Publishers, Dordrecht.

Simitses, G.J., 1987. Instability of dynamically-loaded structures. Appl. Mech. Rev. 40 (10), 1403–1408.

Simitses, G.J., 1990. Dynamic stability of suddenly loaded structures, Springer, New York.

Zhang, Q., Li, S., Zheng, J., 1992. Dynamic response, buckling and collapsing of elastic–plastic straight columns under axial solid–fluid slamming compression–I. experiments.. Int. J. Solids Struct. 29 (3), 381–397.